



Disproportionation or combination? The termination of acrylate radicals in ATRP

Thomas G. Ribelli, Kyle F. Augustine, Marco Fantin, Pawel Krys, Rinaldo Poli, K. Matyjaszewski

► To cite this version:

Thomas G. Ribelli, Kyle F. Augustine, Marco Fantin, Pawel Krys, Rinaldo Poli, et al.. Disproportionation or combination? The termination of acrylate radicals in ATRP. *Macromolecules*, 2017, 50 (20), pp.7920-7929. <10.1021/acs.macromol.7b01552>. <hal-01940158>

HAL Id: hal-01940158

<https://hal.science/hal-01940158v1>

Submitted on 1 Mar 2021

HAL is a multi-disciplinary open access archive for the deposit and dissemination of scientific research documents, whether they are published or not. The documents may come from teaching and research institutions in France or abroad, or from public or private research centers.

L'archive ouverte pluridisciplinaire **HAL**, est destinée au dépôt et à la diffusion de documents scientifiques de niveau recherche, publiés ou non, émanant des établissements d'enseignement et de recherche français ou étrangers, des laboratoires publics ou privés.



HAL Authorization

Disproportionation or Combination? The Termination of Acrylate Radicals in ATRP

Thomas G. Ribelli,^a Kyle F. Augustine,^a Marco Fantin,^a Pawel Krys,^a Rinaldo Poli,^{*b,c} Krzysztof Matyjaszewski^{*a}

^aDepartment of Chemistry, Carnegie Mellon University, 4400 Fifth Avenue, Pittsburgh, Pennsylvania 15213, USA

^bCNRS, LCC (Laboratoire de Chimie de Coordination), Université de Toulouse, UPS, INPT, 205 Route de Narbonne, BP 44099, F-31077, Toulouse Cedex 4, France

^cInstitut Universitaire de France, 1, rue Descartes, 75231 Paris Cedex 05, France

ABSTRACT

The termination of acrylate radicals in atom transfer radical polymerization (ATRP) can involve either conventional bimolecular radical termination (RT) or catalytic radical termination (CRT). These processes were investigated using a poly(methyl acrylate)-Br macroinitiator under different initial conditions tuned to change the RT/CRT ratio. The polymers, obtained from alkyl halide chain-end activation by $[\text{Cu}^{\text{I}}(\text{L})]^+$ ($\text{L} = \text{tris}[\text{2-(dimethylamino)ethyl}]\text{amine (Me}_6\text{TREN)}$, $\text{tris(2-pyridylmethyl)amine (TPMA)}$, or $\text{tris(3,5-dimethyl-4-methoxy-2-pyridylmethyl)amine (TPMA}^{\text{*3}})$) in the absence of monomer, were analyzed by size exclusion chromatography (SEC). RT-promoting conditions resulted in the increase of a shoulder with double molecular weight (MW) relative to the macroinitiator distribution, indicating that RT occurred predominantly via radical combination. Conversely, when CRT was promoted, the macroinitiator distribution did not shift, indicating a disproportionation-like pathway. The termination reactions for the TPMA system were further analyzed via PREDICI simulations, which showed the significant impact of mid-chain radicals, arising from backbiting, on the overall termination profile. In all cases, CRT and cross termination between secondary chain-end and tertiary mid-chain radicals contributed the most to the overall amount of terminated chains.

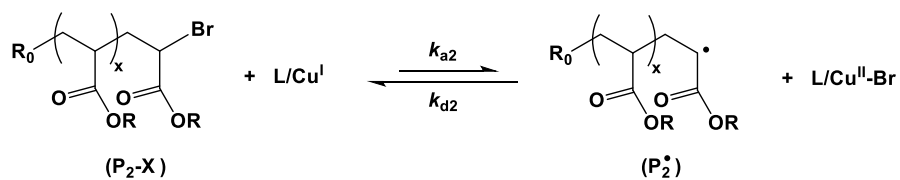
INTRODUCTION

Conventional radical polymerization (RP) and the recently developed reversible-deactivation radical polymerization (RDRP) methods have achieved tremendous success.¹⁻⁵ Versatility of the radical-based processes originates from facile experimental setup, wide range of reaction temperatures, and tolerance to functional groups, solvents, and impurities. Throughout the years, elementary reactions occurring in radical polymerizations have been identified and meticulously studied.⁶⁻¹¹ This also led to development of sophisticated techniques allowing for the precise determination of rate coefficients.^{7, 12-13} In conventional RP, propagation and termination rate coefficients can be accurately measured using time-resolved electron paramagnetic resonance (EPR) spectroscopy coupled with single pulse pulsed laser polymerization technique (SP-PLP).¹⁴⁻²⁰ Although the kinetics of termination has been well studied, the mechanism of bimolecular termination is still a topic of some debate.

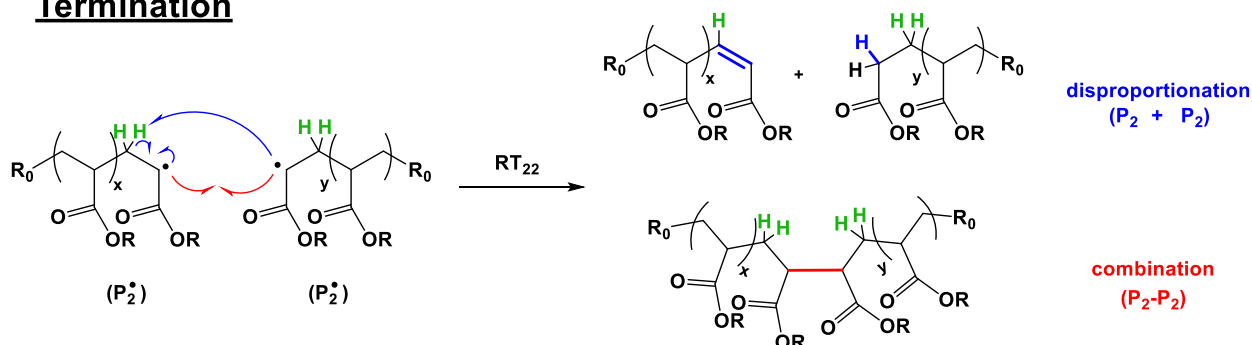
As shown in **Scheme 1**, bimolecular radical termination can occur via combination (Comb) or disproportionation (Disp), resulting in one chain with doubled molecular weight or two chains with a saturated and unsaturated chain end, respectively. The relative extent of these reactions depends on the nature of the radicals. Styrenes²¹⁻²² and acrylonitrile²³ were suggested to primarily undergo coupling, while methacrylates undergo both Disp and Comb^{22, 24}. Acrylates, however, present a more complex, debated, and yet unresolved case.^{21, 25-26} Recently, using radicals photo-generated from organotellurium macroinitiators, Yamago *et al.* suggested that acrylate radicals terminate predominantly (99%) by disproportionation at room temperature.²⁷ Most recently, Yamago *et al.* has published on a surprising temperature and viscosity dependence on the termination mechanism of macro and small molecule RTe-(p)MMA and RTe-(p)St compounds with higher temperature increasing the fraction of combination and higher viscosities promoting combination.²⁸ Because of this, we recently reported on a newly proposed tellanyl catalyzed disproportionation²⁹ to rationalize their results. Asua *et al.*³⁰ also suggested that acrylate radicals terminate via combination, but transfer reactions can also explain the surprising results reported by Yamago. Due to the relatively high reactivity of the acrylate radicals, both intermolecular³¹ and intramolecular (backbiting)³²⁻³³ transfer to polymer can occur.³⁴⁻³⁷ Such reactions lead to tertiary mid-chain radicals (MCR), which

can terminate with another secondary propagating radical (SPR) or MCR.³⁸ At higher temperatures, MCRs undergo radical migration³⁹⁻⁴⁰ and β -scission leading to macromonomers.⁴¹⁻⁴³ Undoubtedly, transfer reactions are important for in-depth understanding of the termination mechanism of acrylates. This also holds true in RDRP techniques, where radical termination is suppressed.

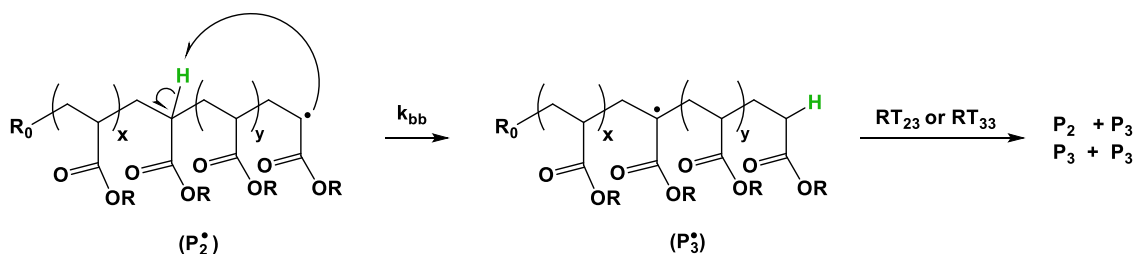
Radical Generation



Termination



Backbiting



Scheme 1 (Top) Pathways of bimolecular radical termination of two chain—end acrylate radicals (P₂[•]), proceeding either via disproportionation (blue) or combination (red); (bottom) formation of tertiary mid-chain radicals (P₃[•]) via backbiting and subsequent termination with another mid-chain radical or secondary chain-end radical, both resulting in disproportionated chains.³⁸

products of CRT as well as obtain valuable information about the mechanism of conventional bimolecular radical termination.

One method of studying termination mechanisms is by generating chain-end radicals via activation of “living” macroinitiators. Using various initial conditions and catalytic systems, we were able to kinetically promote different contributions of conventional radical termination of chain-end radicals (RT) and catalytic radical termination (CRT). By analyzing the kinetics of termination and molecular weights of the resulting polymers, valuable mechanistic insights were obtained. According to **Eq. 1**, to increase the fraction of RT relative to CRT one can: a) decrease $[L/Cu^{II}-X]_0$ or b) increase the ATRP equilibrium constant (K_{ATRP}):

$$\frac{Rate_{RT}}{Rate_{CRT}} = \frac{2k_t[P_n\cdot]^2}{2k_{CRT}[P_n\cdot][L/Cu^I]} = \frac{k_t[P_n\cdot]}{k_{CRT}[L/Cu^I]} = \frac{k_t[P_nX]}{k_{CRT}[L/Cu^{II}-X]} K_{ATRP} \quad (1)$$

Indeed, PREDICI simulations carried out at three different initial conditions confirmed the predictions from **Eq 1**. As shown in **Figure 1**, when using the same catalyst (i.e. same K_{ATRP}), RT_{22}/CRT is higher for a) lower $[PMA-Br]:[L/Cu^I]$ ratio (1:1) and b) lower $[L/Cu^{II}]$. Note that RT_{22} refers to termination between secondary radicals. **Figure 1** also shows the large variation of the RT_{22}/CRT ratio with time. RT_{22}/CRT is largest only at the very first instants when radical concentration is highest. Since the bimolecular termination of chain-end radicals depends on $[R\cdot]^2$, RT_{22} dominates only during the very first milliseconds. Once the $L/Cu^{II}-X$ deactivator builds-up via the persistent radical effect (PRE), the $[R\cdot]$ is suppressed, thus significantly decreasing the rate of RT_{22} . After this initial “influx” of radicals, CRT dominates since $[Cu^I] \gg [R\cdot]$ and thus a radical will preferentially coordinate to L/Cu^I before terminating with a second radical. This is further shown under the most CRT-inducing conditions (green line), where additional deactivator is present from the beginning and a very small RT/CRT is observed, even at the onset of the reaction. This is because the initial influx of radicals can be quickly deactivated before termination. Therefore, since PREDICI confirmed that the RT/CRT ratio can be kinetically controlled by changing the initial conditions, a pMA-Br ATRP macroinitiator with 99%

chain end functionality (CEF; from ^1H NMR, **Figure S1**) was synthesized via Ag^0 ATRP.⁶⁰ By changing the $\text{RT}_{22}/\text{CRT}$ ratio, one can analyze the resulting polymer products via SEC to determine the proportion of high MW to low MW polymer and thus obtain invaluable mechanistic information about the products of RT and CRT.

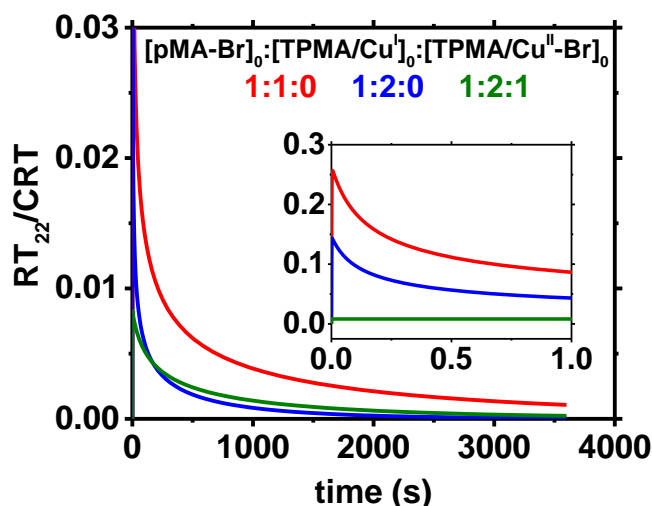


Figure 1. PREDICI simulations of termination of radicals generated from a pMA-Br macroinitiator. $\text{RT}_{22}/\text{CRT}$ ratio vs. time under three different initial conditions $[\text{pMA-Br}]_0:[\text{L/Cu}^{\text{I}}]_0:[\text{L/Cu}^{\text{II-Br}}]_0 = 1:1:0$ (red), $1:2:0$ (blue) and $1:2:1$ (green) where $\text{L} = \text{TPMA}$. The reaction model and rate coefficients used for simulations are presented in **Table S2**.

In order to reassess previous contributions, experiments were first conducted under conditions similar to those reported by Yamago *et al.*²² In order to eliminate assumptions which were not accounted for by Yamago, we slightly altered the experimental setup. One significant difference is the choice of copper salt and solvent. $[\text{Cu}^{\text{I}}(\text{MeCN})_4][\text{PF}_6]$ in acetonitrile was used throughout this study, while Yamago *et al.* used $\text{Cu}^{\text{I}}\text{Br}$ in toluene. In our study, the use of $[\text{Cu}^{\text{I}}(\text{MeCN})_4][\text{PF}_6]$ results in the formation of a discrete $[\text{Cu}^{\text{I}}(\text{Me}_6\text{TREN})]^+$ catalyst *in situ*, while the use of $\text{Cu}^{\text{I}}\text{Br}$ has been shown to form a mixture of $[\text{Cu}^{\text{I}}(\text{Me}_6\text{TREN})]^+$, $[\text{Cu}^{\text{I}}(\text{Me}_6\text{TREN})\text{Br}]$, and $\text{Cu}^{\text{I}}\text{Br}_2^-$, which have different activities in ATRP⁶¹ and thus could have skewed previously reported conclusions. Secondly, to make sure there was no disproportionation of the L/Cu^{I} species, MeCN was chosen as the solvent instead of toluene. Finally, Yamago *et al.* conducted all but one of their termination experiments in the presence of Cu^0 powder, which has recently⁶² been shown to also catalyze the termination of acrylate radicals and would be indistinguishable from

Cu^I CRT. In addition, avoiding the use of Cu⁰ allows facile monitoring of the extent of termination by the determination of [L/Cu^{II}], since Cu⁰ is able to comproportionate with Cu^{II} to regenerate Cu^I and would not allow for efficient monitoring of [L/Cu^{II}].

RESULTS AND DISCUSSION

Termination in the Presence of Me₆TREN/Cu^I Complex

Termination experiments were conducted in the absence of monomer and termination extent could be determined from the increase in [L/Cu^{II}-Br], according to the principle of halogen conservation.⁶³ This allowed the amount of termination to be related to the SEC traces of the resulting terminated polymer (**Figure 2**). Using the same [pMA-Br]₀: [Me₆TREN/Cu^I]₀ = 1:5 as previously reported²², a high molecular weight shoulder accounting for 27% of chains was observed for the polymer recovered after quantitative (>99 %) termination. This is in very good agreement with the Yamago contribution, where 25% of chains were reported to have doubled molecular weight. As predicted by **Eq 1**, upon addition of [Me₆TREN/Cu^{II}-Br]⁺ deactivator, the amount of conventional radical termination was kinetically suppressed relative to CRT. Upon addition of 0.5 or 1 equivalents of [Me₆TREN/Cu^{II}-Br]⁺ relative to [pMA-Br]₀, the fraction of high molecular weight polymer decreased from 27% to 9% and 7%, respectively (in all cases, the termination was quantitative after 1 hour according to the [Me₆TREN/Cu^{II}] analysis). These results would indicate that the high molecular weight peak previously attributed to CRT coupling²² is actually the result of non-catalyzed termination (RT), due to the high radical concentration triggered by fast pMA-Br chain-end activation by the [Cu^I(Me₆TREN)]⁺ catalyst.

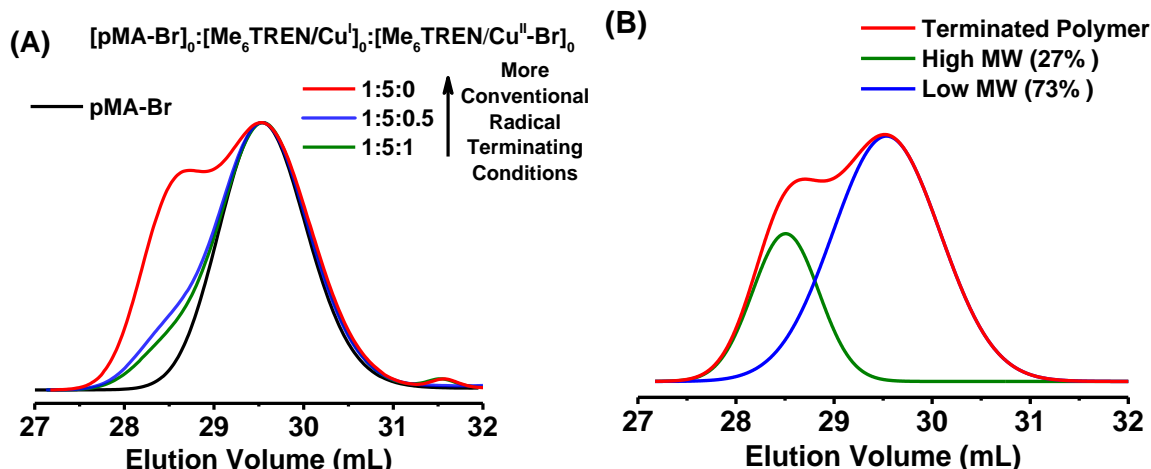


Figure 2 (A) SEC traces of the termination products from the pMA-Br macroinitiator recovered after 30 min at different RT/CRT ratios and (B) deconvolution of the product of reaction $[pMA-Br]:[Me_6TREN/Cu^I] = 1:5$. Conditions: $[pMA-Br]:[Me_6TREN/Cu^I]:[Me_6TREN/Cu^{II}-Br] = 1:5:0-1$ in anhydrous MeCN at room temperature; $[pMA-Br]_0 = 1.6$ mM.

In order to assess the products of RT and CRT under more relevant polymerization conditions, termination reactions under $[pMA-Br]_0:[Me_6TREN/Cu^I]_0 = 1:1-2$ ratios were conducted. The kinetics of termination and the resulting SEC traces of the terminated polymer are presented in **Figure 3**. Under the initial conditions $[pMA-Br]_0:[Me_6TREN/Cu^I]_0 = 1:1$, 81% of chains were terminated after one hour with 38% high molecular weight fraction compared to >99% and 27%, respectively, when this ratio was 1:5. Upon initial addition of 0.5 eq. of deactivator complex $[Me_6TREN/Cu^{II}-Br]^+$ relative to $[pMA-Br]_0$ and doubling $[Me_6TREN/Cu^I]_0$, the high molecular weight shoulder decreased to 18% while achieving 91% termination. The higher amount of terminated chains is due to the excess of $[Me_6TREN/Cu^I]_0$ relative to $[pMA-Br]_0$. The high molecular weight peak was further decreased upon initial addition of 1 eq. of deactivator complex to give only 7% high molecular weight chains at quantitative termination. These results indicate that acrylate radicals terminate via combination, while CRT gives a terminated polymer with the same molecular weight as the pMA-Br macroinitiator, contrary to recent reports.^{22, 27} Due to the high activity of the $[Me_6TREN/Cu^I]$ activator complex, the initial concentration of radicals could not be suppressed efficiently to completely eliminate RT, as evidenced by the small high molecular weight fraction even in the presence of 1 eq. of deactivator complex.

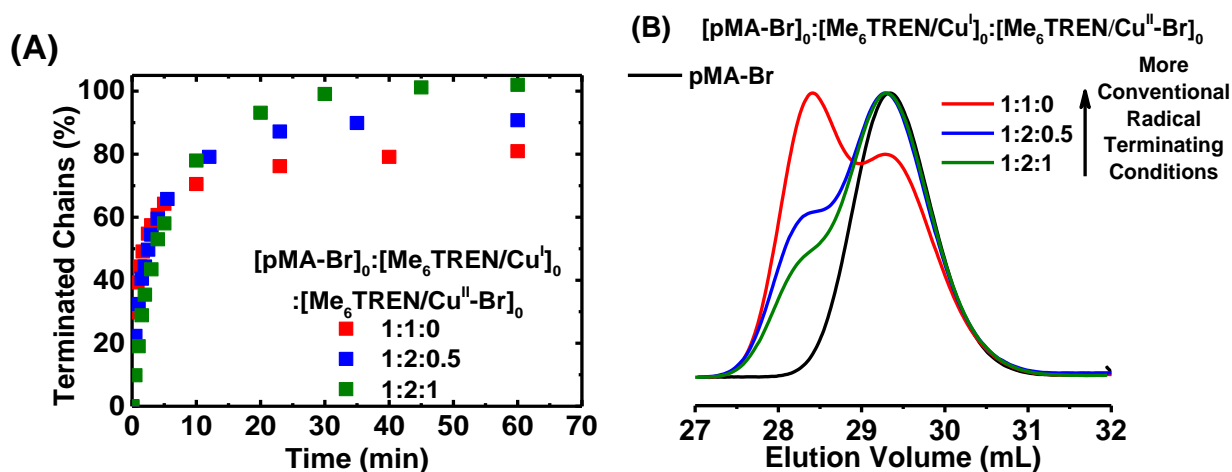


Figure 3 (A) evolution of fraction of terminated chains with time and (B) SEC traces of the termination product of pMA-Br macroinitiator recovered after 30 min at different RT/CRT ratios. Reaction conditions: $[\text{pMA-Br}]_0 : [\text{Me}_6\text{TREN/Cu}^{\text{I}}]_0 : [\text{Me}_6\text{TREN/Cu}^{\text{II}}-\text{Br}]_0 = 1:1:2:0:1$, in anhydrous MeCN at room temperature; $[\text{pMA-Br}]_0 = 1.6 \text{ mM}$.

Termination in the Presence of TPMA/ Cu^{I} Complex

The next termination experiments were carried out using the $[\text{Cu}^{\text{I}}(\text{TPMA})]^+$ (TPMA = tris(2-pyridylmethyl)amine)) catalyst as shown in **Figure 4**. The catalyst was used at two different $[\text{pMA-Br}]_0 : [\text{TPMA/Cu}^{\text{I}}]_0$ ratios. With $[\text{pMA-Br}]_0 : [\text{TPMA/Cu}^{\text{I}}]_0 = 1:1$, 67% of chains were terminated after one hour, but only 7% of all chains corresponded to the high molecular weight shoulder, compared to 38% for the Me_6TREN system under the same conditions. The fraction of high molecular weight terminated polymer was further decreased by decreasing the RT/CRT ratio using different concentration of $[\text{TPMA/Cu}^{\text{I}}]_0$ and $[\text{TPMA/Cu}^{\text{II}}-\text{Br}]_0$. Relative to the Me_6TREN system, the lower fraction of doubled molecular weight product is due to the lower ATRP activity of the TPMA catalyst. The rate coefficient of pMA-Br activation is approximately 10x higher for $[\text{Cu}^{\text{I}}(\text{Me}_6\text{TREN})]^+$ compared to $[\text{Cu}^{\text{I}}(\text{TPMA})]^+$.⁶⁴ Since the rate of radical termination is proportional to $[\text{R}^\bullet]^2$ and the rate of CRT is proportional only to $[\text{R}^\bullet]$, a 10-fold increase in radicals leads to a 100 times faster RT and only 10 times faster CRT.

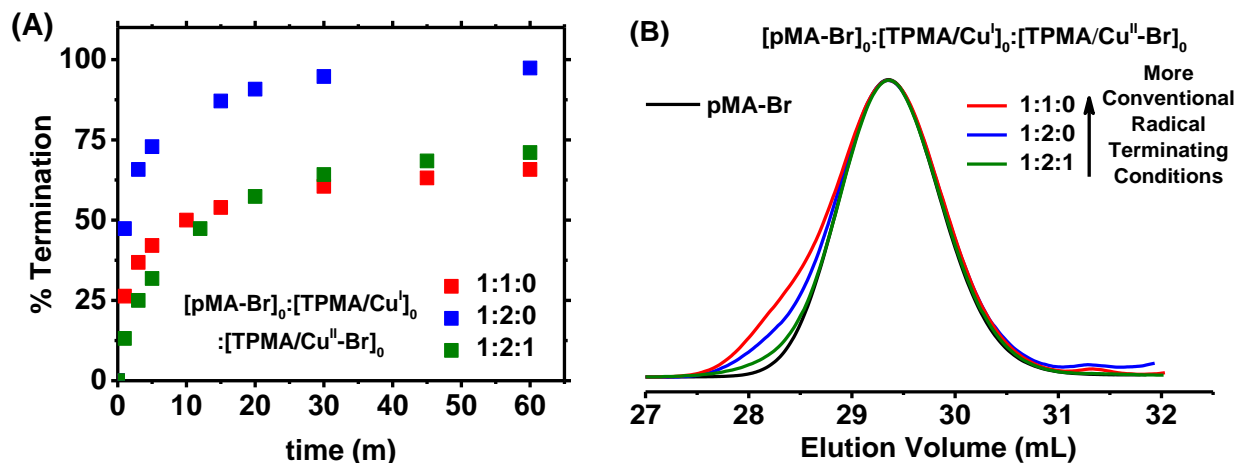


Figure 4 (A) Evolution of fraction of terminated chains with time and (B) SEC trace of the termination product of pMA-Br macroinitiator recovered after 1 h at different RT/CRT ratios. Reaction conditions: $[pMA-Br]_0:[TPMA/Cu^I]_0:[TPMA/Cu^{II}-Br]_0 = 1:1-2:0-1$, in anhydrous MeCN at room temperature; $[pMA-Br]_0 = 2$ mM.

*Termination in the Presence of $Cu^I/TPMA^{*3}$ Complex*

As noted earlier, the ratio of RT to CRT can be tuned by changing K_{ATRP} (**Eq 1**). One way to increase K_{ATRP} is by using more active L/Cu^I catalysts.^{48, 65} In fact, the use of Me₆TREN by Yamago increases K_{ATRP} by approximately 10 compared to the TPMA system reported in **Figure 3**. However, to use geometrically similar pyridinic-based catalysts, $[Cu^I(TPMA)][PF_6]$ was replaced with the more active $[Cu^I(TPMA^{*3})][PF_6]$ ($TPMA^{*3}$ = tris(3,5-dimethyl-4-methoxy-2-pyridylmethyl)amine) catalyst, which should also lead to a higher initial concentration of radicals. As alluded to above, this should lead to a faster rate of RT relative to CRT compared to the TPMA system. Therefore, assuming that RT occurs via combination, as suggested by the investigations of the TPMA and Me₆TREN systems above, a larger fraction of high molecular weight peak should be observed when using $TPMA^{*3}$ compared to TPMA under the same conditions.

Indeed, the termination experiment under conditions $[pMA-Br]_0:[TPMA^{*3}/Cu^I]_0 = 1:1$ (**Figure 5**) confirmed this expectation. After only 5 minutes, 98% of chains were terminated, compared to only 67% after 1 hour for the TPMA system under the same initial conditions. This is due to the much higher activity of the $TPMA^{*3}/Cu^I$ catalyst. Deconvolution of the resulting SEC traces showed 24% of the chains terminated via

combination for TPMA^{*3} compared to only 7% for TPMA. Under the conditions [pMA–Br]₀: [TPMA^{*3}/Cu^I]₀ = 1:2 all chains were terminated in only 4 minutes and the high molecular weight shoulder accounted for only 12% of all chains, indicating a larger fraction of CRT relative to RT. Upon initial addition of 0.5 or 1 equivalent of TPMA^{*3}/Cu^{II}-Br deactivator, the high molecular weight peak decreased to 7 and 4%, respectively, with >99% of chains terminated. The concurrent decrease of the high molecular weight shoulder with decreasing RT provides further evidence that RT occurs predominantly via combination while CRT gives products with the same molecular weight as the pMA-Br macroinitiator. Like in the Me₆TREN system, a small fraction of high molecular weight product was observed due to the high activity of the TPMA^{*3}/Cu^I catalyst.

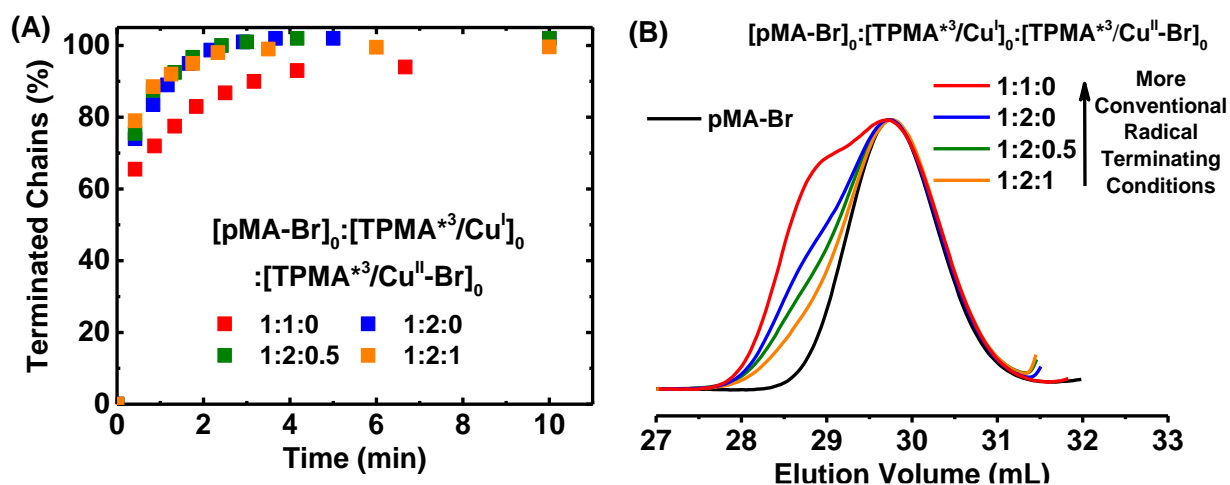


Figure 5 (A) Evolution of fraction of terminated chains with time and (B) SEC traces of the termination product of pMA–Br macroinitiator recovered after 1 h at different RT/CRT ratios. Reaction conditions: [pMA–Br]₀: [TPMA^{*3}/Cu^I]₀: [TPMA^{*3}/Cu^{II}-Br]₀ = 1:1-2:0-1, in anhydrous MeCN at room temperature; [pMA–Br]₀ = 2.5 mM).

An interesting question arises as to why the TPMA^{*3} system did not show as much of a high molecular weight peak as the Me₆TREN system. This is most likely due to much faster association of the pMA radicals to TPMA^{*3}/Cu^I relative to Me₆TREN/Cu^I. In fact, UV-Vis analysis shows the formation of both the TPMA^{*3}/Cu^{II}-Br and the TPMA^{*3}/Cu^{II}-pMA organometallic species (**Figure S5**). Since this organometallic species was observed on the time scale of the reaction, this means that TPMA^{*3}/Cu^{II}-pMA is more thermodynamically stable (larger value of K_{OMRP})⁵⁸ than Me₆TREN/Cu^{II}-pMA. Formation

of TPMA*³/Cu^{II}-pMA decreases the radical concentration, thus suppressing the rate of bimolecular termination and therefore decreasing the fraction of high molecular weight product in SEC.

The summary of all termination reactions (**Table 1**) clearly shows that the RT/CRT ratio can be kinetically altered by changing the [pMA-Br]:[L/Cu^I]:[L/Cu^{II}-Br] ratios but also by changing K_{ATRP} . As the RT/CRT ratio was kinetically decreased, the relative fraction of high molecular polymer (Comb/Disp) also decreased. These results indicate that bimolecular radical termination of acrylates operates predominantly via combination while CRT gives predominantly chains with the same molecular weight as the pMA-Br initiator.

Table 1 Experimental product distribution of the termination reactions.

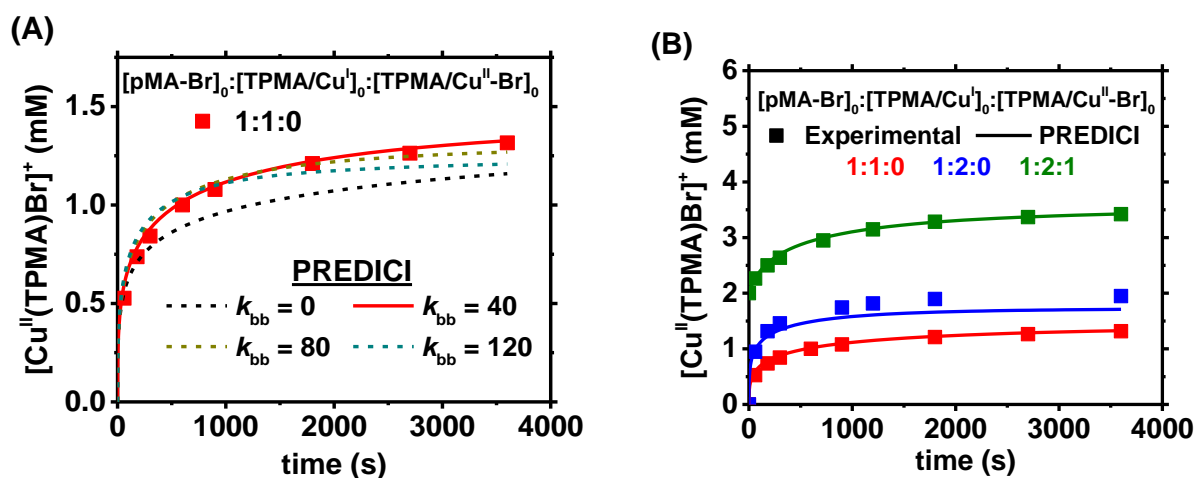
Ligand	[pMA-Br]: [L/Cu ^I]:[L/Cu ^{II} -Br]	Terminated (%) ^a	Living (%)	Combined (%) ^b	Disp (%) ^c	% Disp. Of All Term ^d
Me ₆ TREN	1:1:0	81	19	38	43	53
	1:2:0.5	91	9	18	73	80
	1:2:1	>99	<1	13	86	86
	1:5:0	>99	<1	27	73	73
	1:5:0.5	>99	<1	9	91	91
	1:5:1	>99	<1	7	93	93
TPMA	1:1:0	67	33	7	60	90
	1:2:0	98	2	5	93	95
	1:2:1	71	29	2	69	97
TPMA* ³	1:1:0	98	2	24	74	76
	1:2:0	>99	<1	12	88	88
	1:2:0.5	>99	<1	7	93	93
	1:2:1	>99	<1	4	96	96

All percentages were calculated at $t = 30$ min (TPMA*³) or 1 h (TPMA and Me₆TREN); Relative to [pMA-Br]₀ unless otherwise noted. ^a Calculated based on the increase of [L/Cu^{II}-Br]; ^b The High MW from the deconvoluted SEC traces; ^c Calculated from the Low MW fraction of the deconvoluted SEC traces as Low MW = Living + Disp; ^d Calculated as the amount of chains terminated by disproportionation related to all terminated chains.

PREDICI Simulations

To further quantify the termination reactions, PREDICI simulations were conducted. In order to obtain useful mechanistic information, the kinetic model in use must first be validated by comparing to experimental results. In this case, experimental $[L/Cu^{II}-Br]$ was conveniently monitored by UV-Vis spectroscopy and then compared to the PREDICI simulations.

One major area of debate in the termination of acrylate radicals is the extent of backbiting for which reported rate coefficients, k_{bb} , span 4 orders of magnitude at the same temperature.³⁸ However, backbiting is an important feature of acrylate polymerization and cannot be neglected.³² In fact, setting $k_{bb} = 0$ in the simulation (**Figure 6A**) caused a significant underestimation of the experimental $[L/Cu^{II}-Br]$. Therefore, backbiting was included in the simulation, taking into account the most recent and accurate k_{bb} value at room temperature reported by Buback *et al.*^{16, 33} using the PLP-SEC or PLP-EPR methods ($40 < k_{bb} < 250$) and Asua *et al.*³⁸ using experimental fitting ($10 < k_{bb} < 40$) also at room temperature. With k_{bb} in this range, all simulations agreed better with the experimental data, and the best agreement was obtained for $k_{bb} = 40 \text{ s}^{-1}$ at room temperature. It should be noted that the value of k_{bb} , within its interval of accuracy, was the only value fitted to the experimental data, whereas all other values were taken directly from the literature or measured in this study (see **Supporting Information**).



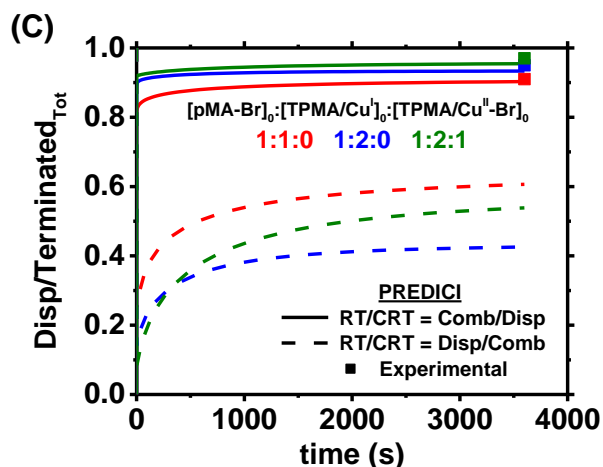


Figure 6 A) Evolution of $[\text{TPMA/Cu}^{\text{II}}\text{-Br}]$ vs. time for different values of k_{bb} (in s^{-1}); B) experimental (squares) and simulated (lines) evolution of $\text{TPMA/Cu}^{\text{II}}\text{-Br}$ vs. time; C) fraction of chains terminated by disproportionation relative to total terminated chains for two cases, where RT and CRT give combination and disproportionation, respectively (bold lines) and vice versa (dashed lines). All squares are experimental data obtained either via UV-Vis or SEC under the specified initial ratio with $[\text{pMA-Br}]_0 = 2 \text{ mM}$ in anhydrous MeCN at room temperature.

The remaining simulations were conducted using the value of $k_{\text{bb}} = 40 \text{ s}^{-1}$. As shown in **Figure 6B**, the fit between the experimental and simulated evolution of $\text{TPMA/Cu}^{\text{II}}\text{-Br}$ for the other two $[\text{pMA-Br}]:[\text{L/Cu}^{\text{II}}\text{-Br}]$ ratios remained good, validating this PREDICI model. **Figure 6C** shows the fraction of disproportionated chains to total terminated chains vs. time under two different scenarios. In the bold lines, it was assumed that termination between two chain-end radicals (RT_{22}) gives 100% Comb while CRT gives 100% Disp. On the other hand, in the dashed lines, the assumptions were reversed, in which case RT_{22} gives 100% disproportionation and CRT gives 100% combination, as has been proposed by Yamago.^{22, 27}

The extent of Disp/Comb for the mid-chain radical is not precisely known and has only been taken as the average of RT_{22} and RT_{33} .⁶⁶ In light of this and due to the best fitting between experimental and PREDICI, it was assumed that any termination involving tertiary mid-chain radicals (RT_{23} and RT_{33}) gives 100% disproportionation.^{36, 38} In fact, Asua *et al*⁶⁰ has proposed that the study conducted by Yamago *et al*²⁷ more accurately models how tertiary mid-chain radicals terminate as opposed to chain-end radicals due

to $[P_3\bullet] > [P_2\bullet]$. This gives further support of bimolecular termination involving mid-chain radicals terminating by disproportionation at room temperature. The experimental results can only be explained if one assumes that RT_{22} operates via combination while CRT gives products of disproportionation. This further validates the experiments conducted above, in which reactions that were kinetically tuned to promote RT vs. CRT gave a higher molecular weight shoulder.

To quantify the contribution of each reaction toward the decrease in chain-end functionality, the evolution of all products of termination were simulated with respect to time. In the present model, there are four pathways in which radicals can terminate: 1) CRT, the reaction between TPMA/Cu^{II}-P₂ and a chain-end radical, P₂[•]; 2) RT_{22} , the reaction between two chain-end radicals; 3) RT_{23} , the “cross-termination” between a chain-end radical and a mid-chain radical; 4) RT_{33} , the reaction between two mid-chain radicals. Based on the good fit between experimental and simulations in **Figure 6C**, the three reactions CRT, RT_{23} and RT_{33} were simulated to give disproportionated chains and RT_{22} was set to give combined chains. **Figure 7** shows the distribution of products obtained by these four termination reactions.

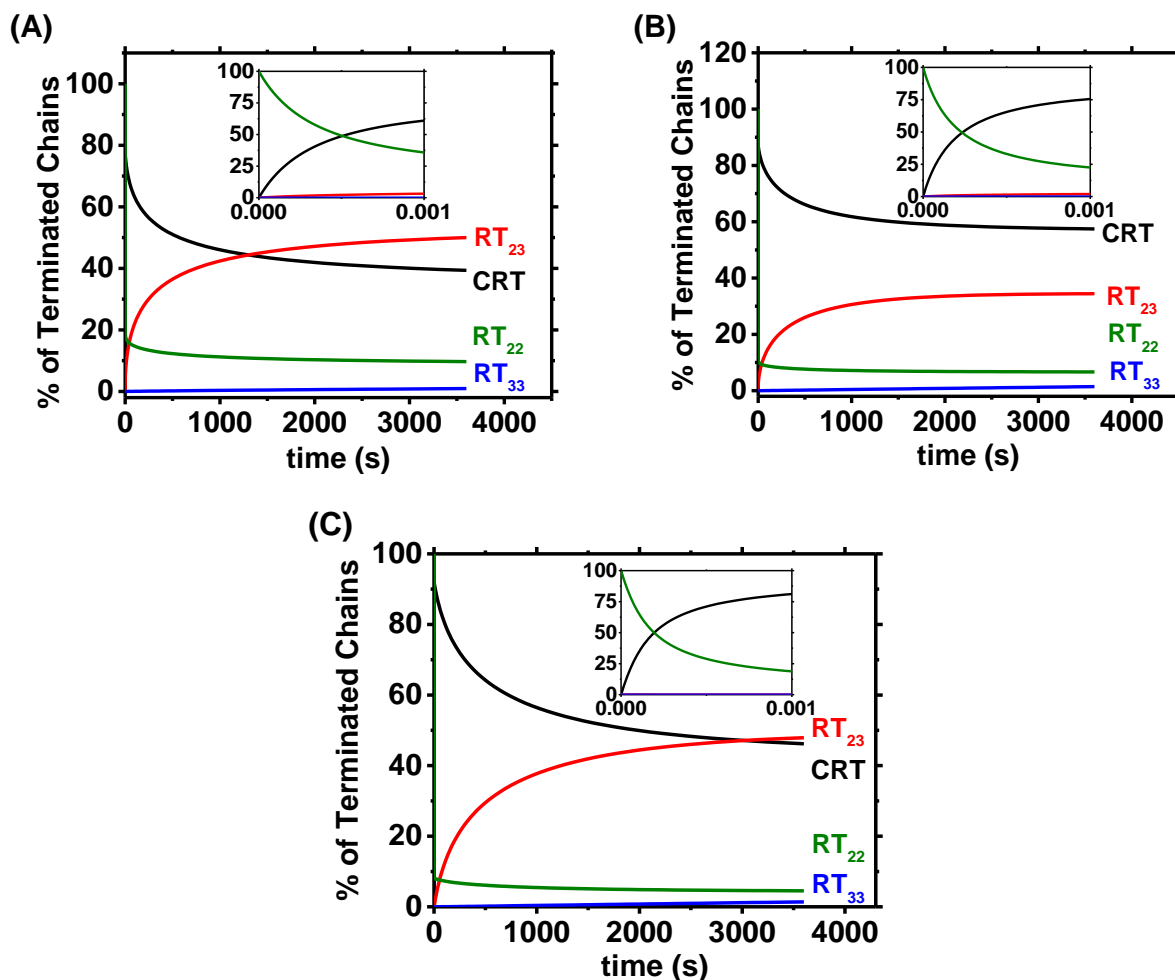


Figure 7 Simulations of the contribution of CRT (black), RT₂₃ (red), RT₂₂ (green) and RT₃₃ (blue) to total termination vs. time under the initial [pMA-Br]₀:[TPMA/Cu^I]₀:[TPMA/Cu^{II}-Br]₀ ratios of (A) 1:1:0 (B) 1:2:0 and (C) 1:2:1 at room temperature. The reaction model and rate coefficients used for simulations are presented in **Table S2**.

For the ratio [pMA-Br]₀:[TPMA/Cu^I]₀:[TPMA/Cu^{II}-Br]₀ = 1:1:0 (**Figure 7A**), a surprising result is the dominance of the bimolecular “cross termination” between chain-end and mid-chain radicals (RT₂₃). So much, in fact, that after approximately 25 minutes, the majority of terminated chains underwent termination via cross termination. The reasoning becomes apparent when looking at **Figure S5B** which shows that the concentration of tertiary mid-chain radicals (P₃[•]) was greater than that of secondary chain-end radicals (P₂[•]) after only 5 minutes. This relatively higher concentration of mid-chain radicals results from the fast rate of backbiting (BB) as shown in **Figure S5D**. In fact, backbiting was between 10 and 100 times faster than RT₂₂ due to the unimolecular nature of the reaction.

The high abundance of mid-chain radicals in acrylate polymerization has previously been observed via EPR even at room temperature.³² PREDICI simulations showed that after one hour, 50% of all terminated chains were terminated via RT_{23} while surprisingly only 39% were terminated via CRT. Only within the first millisecond of the reaction, when $[P_2^*]$ was highest (**Figure S5A**), did RT_{22} dominate RT_{23} , as shown in the insert in **Figure 7A**. Finally, due to the slower reaction between two sterically hindered mid-chain radicals, RT_{33} accounted for only 1% of all terminated chains.

The simulations under the more CRT promoting conditions of $[pMA-Br]_0:[TPMA/Cu^I]_0:[TPMA/Cu^{II}-Br]_0 = 1:2:0$ were similar to those using the 1:1:0 ratio, since the initial ratio of RT and CRT rates does not depend on $[TPMA/Cu^{II}-Br]_0$ (Equation 1). However, relatively more chains were terminated via CRT. This is due to a two-fold effect of the excess TPMA/Cu^I on the overall rate of termination. Firstly, the faster P_2^* trapping by TPMA/Cu^I suppressed chain-end radical concentration thus slowing down the backbiting reaction (**Figure S6**) and suppressing the rate of cross-termination, RT_{23} , by an order of magnitude. Secondly, this caused a slight initial increase in $[TPMA/Cu^{II}-P]$, which resulted in a faster increase of the CRT rate as shown in **Figure S6D**. Under these initial conditions, CRT accounted for 57% of all terminated chains compared to 39% for the 1:1:0 ratio. Furthermore, at this 1:2:0 ratio, 7% of chains were terminated via RT_{22} compared to 10% under the 1:1:0 ratio, as expected according to **Figure 1**. Nonetheless, RT_{23} still dominated all bimolecular radical-based termination events, accounting for 34% of all terminated chains.

Using the initial ratio $[pMA-Br]_0:[TPMA/Cu^I]_0:[TPMA/Cu^{II}-Br]_0 = 1:2:1$, only 4% of chains were terminated via RT_{22} . This is because the concentration of chain-end radicals was significantly suppressed by the quick and efficient trapping by the TPMA/Cu^{II}-Br deactivator present from the beginning. As shown in **Figure S7C**, after one second, the concentration of chain-end radicals was $[P_2^*] \approx 7 \times 10^{-8}$ M in the presence of the deactivator. In comparison, after one second but in the absence of initially added deactivator, $[P_2^*] \approx 3 \times 10^{-7}$ M as shown in **Figure S6A**. Interestingly, the amount of CRT and RT_{23} were 46% and 48%, respectively. Under these “most CRT promoting

conditions,” one would have expected the most amount of CRT according to **Eq 1**. This can be rationalized on the basis that the initial rate of CRT is suppressed by a factor of 50 due to the suppression of $[P_2^*]$ by the initially added TPMA/Cu^{II}-Br deactivator. Since CRT requires the reaction between TPMA/Cu^{II}-P₂ and $[P_2^*]$, the suppression of the latter will undoubtedly slow down the rate of CRT. Although the “most CRT-promoting conditions” did in fact lead to the most amount of disproportionation, they did not result in the most amount of chains being terminated via CRT. Thus, **Eq 1** would be better referenced as a way to kinetically suppress RT₂₂ as opposed to kinetically promote CRT. The summary of the distribution of terminated polymer according to our simulations are summarized in **Table 2**.

It should be noted that in the case of a polymerization reaction, the mid-chain radicals can also add to acrylate monomer leading to a branching point and regenerate the secondary chain-end radical. This could significantly decrease the concentration of mid-chain radicals and increase the concentration of chain-end radicals compared to this study. This would presumably decrease the contribution of RT₂₃ and RT₃₃ while increasing the contribution of RT₂₂ and CRT. Nonetheless, in “termination reactions” the lack of monomer allows for a build-up of MCRs and thus bimolecular radical termination involving MCRs cannot be neglected.

Table 2 Product distribution of terminated polymer chains.

[pMA-Br]: [L/Cu ^I]:[L/Cu ^{II} -Br]	CRT (%)	RT ₂₃ (%)	RT ₃₃ (%)	RT ₂₂ (%)
1:1:0	39	50	1	10
1:2:0	57	34	2	7
1:2:1	46	48	2	4

All percentages were calculated based on total terminated chains $Term_{tot} = [CRT] + [RT_{23}] + [RT_{33}] + 2*[RT_{22}]$ since chains undergoing combination comprise two initial pMA-Br macroinitiators. For all cases L = TPMA.

The results presented here indicate that RT₂₂ operates predominately via combination whereas CRT gives products with the same molecular weight as the living chain. This is in direct contrast to the previous contribution by Yamago *et al.*, which concluded that

acrylate chain-end termination occurs predominately (>99%) via disproportionation²⁷ while CRT gives coupling.²² In order to rationalize the results observed with the organotellurium systems studied by Yamago, we have disclosed $\bullet\text{TeR}$ radical catalyzed disproportionation via an H-TeR intermediate.²⁹ Due to the incorrect assumption that acrylate radicals terminate exclusively via disproportionation at room temperature, it seems that Yamago et al have erroneously assigned the formation of the observed combination products to copper catalyzed termination. The high molecular weight in that study²² is actually the result of conventional radical termination via combination.

CONCLUSIONS

Termination reactions using a pMA-Br ATRP macroinitiator were utilized to shed light on the termination mechanism of polyacrylates in ATRP. Three different catalysts were used under various conditions to change the fraction of bimolecular chain-end radical termination (RT) to copper-catalyzed radical termination (CRT). Wherever the RT/CRT ratio was largest, a high molecular weight shoulder became apparent in the SEC traces. As this ratio was gradually decreased, the relative fraction of high molecular weight polymer decreased significantly. This indicates that the bimolecular radical termination of acrylates operates via combination while CRT gives terminated polymers of unchanged molecular weight. These results are in stark contrast to recent reports; therefore, PREDICI simulations were conducted to support our experimental findings. In fact, very similar results were observed for the experimental and simulated data for the TPMA-based system. It was found that due to the high initial radical concentration, bimolecular termination dominated only at the very first instants. After this initial influx of radicals, catalytic radical termination and backbiting dominated the fate of the secondary chain-end radical. Due to the relatively high concentration of mid-chain radicals relative to chain-end radicals, the amount of cross termination between mid-chain and chain-end radicals (RT_{23}) was found to be more dominant than termination via two chain-ends (RT_{22}) and, in some cases, even more kinetically significant than CRT.

AUTHOR INFORMATION

Corresponding Authors:

*(R.P.) Email: rinaldo.poli@lcc-toulouse.fr

*(K.M.) Email: km3b@andrew.cmu.edu

Notes

The authors declare no competing financial interest.

ACKNOWLEDGEMENTS

Support from the NSF (CHE 1707490) is acknowledged. We thank the Centre National de la Recherche Scientifique (CNRS) for support through the PICS06782 grant and through the Laboratoire International Associé (LIA) "Laboratory of Coordination Chemistry for Controlled Radical Polymerization". We are also grateful to the French Embassy in Washington D.C. for a Chateaubriand Fellowship to T.R. P.K. acknowledges Dr. Konrad M. Weis Fellowship in Chemistry. Finally we would like to acknowledge Prof. Michael Buback for fruitful discussion and seminal ideas for this work.

REFERENCES

1. Nicolas, J.; Guillaneuf, Y.; Lefay, C.; Bertin, D.; Gigmes, D.; Charleux, B., Nitroxide-mediated polymerization. *Progress in Polymer Science* **2013**, *38* (1), 63-235.
2. Moad, G.; Rizzardo, E.; Thang, S. H., Living Radical Polymerization by the RAFT Process. *Australian Journal of Chemistry* **2005**, *58* (6), 379-410.
3. Matyjaszewski, K., Atom Transfer Radical Polymerization (ATRP): Current Status and Future Perspectives. *Macromolecules (Washington, DC, United States)* **2012**, *45* (10), 4015-4039.
4. Matyjaszewski, K.; Xia, J., Atom Transfer Radical Polymerization. *Chemical Reviews* **2001**, *101* (9), 2921-2990.
5. Matyjaszewski, K.; Tsarevsky, N. V., Macromolecular Engineering by Atom Transfer Radical Polymerization. *Journal of the American Chemical Society* **2014**, *136* (18), 6513-6533.
6. Krys, P.; Matyjaszewski, K., Kinetics of Atom Transfer Radical Polymerization. *European Polymer Journal* **2017**, *89*, 482-523.
7. Barner-Kowollik, C.; Buback, M.; Egorov, M.; Fukuda, T.; Goto, A.; Olaj, O. F.; Russell, G. T.; Vana, P.; Yamada, B.; Zetterlund, P. B., Critically evaluated termination rate coefficients for free-radical polymerization: Experimental methods. *Progress in Polymer Science* **2005**, *30* (6), 605-643.
8. Moad, G.; Solomon, D. H., 1 - Introduction. In *The Chemistry of Radical Polymerization (Second Edition)*, Elsevier Science Ltd: Amsterdam, 2005; pp 1-9.
9. Buback, M.; Egorov, M.; Gilbert, R. G.; Kaminsky, V.; Olaj, O. F.; Russell, G. T.; Vana, P.; Zifferer, G., Critically Evaluated Termination Rate Coefficients for Free-Radical Polymerization, 1. The Current Situation. *Macromolecular Chemistry and Physics* **2002**, *203* (18), 2570-2582.

10. Beuermann, S.; Buback, M.; Davis, T. P.; García, N.; Gilbert, R. G.; Hutchinson, R. A.; Kajiwar, A.; Kamachi, M.; Lacík, I.; Russell, G. T., Critically Evaluated Rate Coefficients for Free-Radical Polymerization, 4. *Macromolecular Chemistry and Physics* **2003**, *204* (10), 1338-1350.
11. Beuermann, S.; Buback, M.; Davis, T. P.; Gilbert, R. G.; Hutchinson, R. A.; Olaj, O. F.; Russell, G. T.; Schweer, J.; van Herk, A. M., Critically evaluated rate coefficients for free-radical polymerization, 2.. Propagation rate coefficients for methyl methacrylate. *Macromolecular Chemistry and Physics* **1997**, *198* (5), 1545-1560.
12. Fantin, M.; Isse, A. A.; Matyjaszewski, K.; Gennaro, A., ATRP in Water: Kinetic Analysis of Active and Super-Active Catalysts for Enhanced Polymerization Control. *Macromolecules* **2017**, *50* (7), 2696-2705.
13. Tang, W.; Matyjaszewski, K., Effect of Ligand Structure on Activation Rate Constants in ATRP. *Macromolecules* **2006**, *39* (15), 4953-4959.
14. Kattner, H.; Buback, M., Detailed Investigations into Radical Polymerization Kinetics by Highly Time-Resolved SP-PLP-EPR. *Macromolecular Symposia* **2013**, *333* (1, Polymer Reaction Engineering), 11-23.
15. Buback, M.; Schroeder, H.; Kattner, H., Detailed Kinetic and Mechanistic Insight into Radical Polymerization by Spectroscopic Techniques. *Macromolecules* **2016**, *49* (9), 3193-3213.
16. Barth, J.; Buback, M., SP-PLP-EPR-A Novel Method for Detailed Studies into the Termination Kinetics of Radical Polymerization. *Macromolecular Reaction Engineering* **2010**, *4* (5), 288-301.
17. Buback, M.; Egorov, M.; Junkers, T.; Panchenko, E., Free-Radical Termination Kinetics Studied Using a Novel SP-PLP-ESR Technique. *Macromolecular Rapid Communications* **2004**, *25* (10), 1004-1009.
18. Olaj, O. F.; Bitai, I.; Hinkelmann, F., The laser-flash-initiated polymerization as a tool of evaluating (individual) kinetic constants of free-radical polymerization, 2. The direct determination of the rate of constant of chain propagation. *Die Makromolekulare Chemie* **1987**, *188* (7), 1689-1702.
19. Buback, M.; Gilbert, R. G.; Russell, G. T.; Hill, D. J. T.; Moad, G.; O'Driscoll, K. F.; Shen, J.; Winnik, M. A., Consistent values of rate parameters in free radical polymerization systems. II. Outstanding dilemmas and recommendations. *Journal of Polymer Science Part A: Polymer Chemistry* **1992**, *30* (5), 851-863.
20. Beuermann, S.; Buback, M., Rate coefficients of free-radical polymerization deduced from pulsed laser experiments. *Progress in Polymer Science* **2002**, *27* (2), 191-254.
21. Bamford, C. H.; Jenkins, A. D., Termination Reaction in Vinyl Polymerization: Preparation of Block Copolymers. *Nature* **1955**, *176* (4471), 78-78.
22. Nakamura, Y.; Ogihara, T.; Yamago, S., Mechanism of Cu(I)/Cu(0)-Mediated Reductive Coupling Reactions of Bromine-Terminated Polyacrylates, Polymethacrylates, and Polystyrene. *ACS Macro Letters* **2016**, *5* (2), 248-252.
23. Bamford, C. H.; Dyson, R. W.; Eastmond, G. C., Network formation IV. The nature of the termination reaction in free-radical polymerization. *Polymer* **1969**, *10*, 885-899.
24. Buback, M.; Günzler, F.; Russell, G. T.; Vana, P., Determination of the Mode of Termination in Radical Polymerization via Mass Spectrometry. *Macromolecules* **2009**, *42* (3), 652-662.
25. Ayrey, G.; Humphrey, M. J.; Poller, R. C., Radiochemical studies of free-radical vinyl polymerizations: 7. Polymerization of methyl acrylate. *Polymer* **1977**, *18* (8), 840-844.

26. Szablan, Z.; Junkers, T.; Koo, S. P. S.; Lovestead, T. M.; Davis, T. P.; Stenzel, M. H.; Barner-Kowollik, C., Mapping Photolysis Product Radical Reactivities via Soft Ionization Mass Spectrometry in Acrylate, Methacrylate, and Itaconate Systems. *Macromolecules* **2007**, *40* (19), 6820-6833.
27. Nakamura, Y.; Lee, R.; Coote, M. L.; Yamago, S., Termination Mechanism of the Radical Polymerization of Acrylates. *Macromolecular Rapid Communications* **2016**, *37* (6), 506-513.
28. Nakamura, Y.; Ogihara, T.; Hatano, S.; Abe, M.; Yamago, S., Control of the Termination Mechanism in Radical Polymerization by Viscosity: Selective Disproportionation in Viscous Media. *Chemistry – A European Journal* **2017**, *23* (6), 1299-1305.
29. Ribelli, T. G.; Rahaman, W.; Matyjaszewski, K.; Poli, R., Catalyzed Radical Termination in the Presence of Tellanyl Radicals. *Chemistry – A European Journal*, ASAP.
30. Ballard, N.; Hamzehlou, S.; Ruipérez, F.; Asua, J. M., On the Termination Mechanism in the Radical Polymerization of Acrylates. *Macromolecular Rapid Communications* **2016**, *37* (16), 1364-1368.
31. Plessis, C.; Arzamendi, G.; Leiza, J. R.; Schoonbrood, H. A. S.; Charmot, D.; Asua, J. M., Modeling of Seeded Semibatch Emulsion Polymerization of n-BA. *Industrial & Engineering Chemistry Research* **2001**, *40* (18), 3883-3894.
32. Buback, M.; Hesse, P.; Junkers, T.; Sergeeva, T.; Theis, T., PLP Labeling in ESR Spectroscopic Analysis of Secondary and Tertiary Acrylate Propagating Radicals. *Macromolecules* **2008**, *41* (2), 288-291.
33. Nikitin, A. N.; Hutchinson, R. A.; Buback, M.; Hesse, P., Determination of Intramolecular Chain Transfer and Midchain Radical Propagation Rate Coefficients for Butyl Acrylate by Pulsed Laser Polymerization. *Macromolecules* **2007**, *40* (24), 8631-8641.
34. Yu-Su, S. Y.; Sun, F. C.; Sheiko, S. S.; Konkolewicz, D.; Lee, H.-i.; Matyjaszewski, K., Molecular Imaging and Analysis of Branching Topology in Polyacrylates by Atomic Force Microscopy. *Macromolecules* **2011**, *44* (15), 5928-5936.
35. Ahmad, N. M.; Charleux, B.; Farcet, C.; Ferguson, C. J.; Gaynor, S. G.; Hawket, B. S.; Heatley, F.; Klumperman, B.; Konkolewicz, D.; Lovell, P. A.; Matyjaszewski, K.; Venkatesh, R., Chain Transfer to Polymer and Branching in Controlled Radical Polymerizations of n-Butyl Acrylate. *Macromolecular Rapid Communications* **2009**, *30* (23), 2002-2021.
36. Konkolewicz, D.; Sosnowski, S.; D'hooge, D. R.; Szymanski, R.; Reyniers, M.-F.; Marin, G. B.; Matyjaszewski, K., Origin of the Difference between Branching in Acrylates Polymerization under Controlled and Free Radical Conditions: A Computational Study of Competitive Processes. *Macromolecules* **2011**, *44* (21), 8361-8373.
37. Konkolewicz, D.; Krys, P.; Matyjaszewski, K., Explaining Unexpected Data via Competitive Equilibria and Processes in Radical Reactions with Reversible Deactivation. *Accounts of Chemical Research* **2014**, *47* (10), 3028-3036.
38. Hamzehlou, S.; Ballard, N.; Reyes, Y.; Aguirre, A.; Asua, J. M.; Leiza, J. R., Analyzing the discrepancies in the activation energies of the backbiting and [small beta]-scission reactions in the radical polymerization of n-butyl acrylate. *Polymer Chemistry* **2016**, *7* (11), 2069-2077.
39. Vandenbergh, J.; Junkers, T., Macromonomers from AGET Activation of Poly(n-butyl acrylate) Precursors: Radical Transfer Pathways and Midchain Radical Migration. *Macromolecules* **2012**, *45* (17), 6850-6856.

40. Van Steenberge, P. H. M.; Vandenberghe, J.; Reyniers, M.-F.; Junkers, T.; D'hooge, D. R.; Marin, G. B., Kinetic Monte Carlo Generation of Complete Electron Spray Ionization Mass Spectra for Acrylate Macromonomer Synthesis. *Macromolecules* **2017**, *50* (7), 2625-2636.
41. Chiefari, J.; Jeffery, J.; Mayadunne, R. T. A.; Moad, G.; Rizzardo, E.; Thang, S. H., Chain Transfer to Polymer: A Convenient Route to Macromonomers. *Macromolecules* **1999**, *32* (22), 7700-7702.
42. Junkers, T.; Barner-Kowollik, C., Optimum Reaction Conditions for the Synthesis of Macromonomers Via the High-Temperature Polymerization of Acrylates. *Macromolecular Theory and Simulations* **2009**, *18* (7-8), 421-433.
43. Peck, A. N. F.; Hutchinson, R. A., Secondary Reactions in the High-Temperature Free Radical Polymerization of Butyl Acrylate. *Macromolecules* **2004**, *37* (16), 5944-5951.
44. Jakubowski, W.; Matyjaszewski, K., Activators Regenerated by Electron Transfer for Atom-Transfer Radical Polymerization of (Meth)acrylates and Related Block Copolymers. *Angewandte Chemie* **2006**, *118* (27), 4594-4598.
45. Xia, J.; Gaynor, S. G.; Matyjaszewski, K., Controlled/"Living" Radical Polymerization. Atom Transfer Radical Polymerization of Acrylates at Ambient Temperature. *Macromolecules* **1998**, *31* (17), 5958-5959.
46. Chiefari, J.; Chong, Y. K.; Ercole, F.; Krstina, J.; Jeffery, J.; Le, T. P. T.; Mayadunne, R. T. A.; Meijs, G. F.; Moad, C. L.; Moad, G.; Rizzardo, E.; Thang, S. H., Living Free-Radical Polymerization by Reversible Addition-Fragmentation Chain Transfer: The RAFT Process. *Macromolecules* **1998**, *31* (16), 5559-5562.
47. Chong, Y. K.; Krstina, J.; Le, T. P. T.; Moad, G.; Postma, A.; Rizzardo, E.; Thang, S. H., Thiocarbonylthio Compounds [SC(Ph)S-R] in Free Radical Polymerization with Reversible Addition-Fragmentation Chain Transfer (RAFT Polymerization). Role of the Free-Radical Leaving Group (R). *Macromolecules* **2003**, *36* (7), 2256-2272.
48. Schröder, K.; Mathers, R. T.; Buback, J.; Konkolewicz, D.; Magenau, A. J. D.; Matyjaszewski, K., Substituted Tris(2-pyridylmethyl)amine Ligands for Highly Active ATRP Catalysts. *ACS Macro Letters* **2012**, *1* (8), 1037-1040.
49. Schröder, K.; Konkolewicz, D.; Poli, R.; Matyjaszewski, K., Formation and Possible Reactions of Organometallic Intermediates with Active Copper(I) Catalysts in ATRP. *Organometallics* **2012**, *31* (22), 7994-7999.
50. Wang, Y.; Soerensen, N.; Zhong, M.; Schroeder, H.; Buback, M.; Matyjaszewski, K., Improving the "Livingness" of ATRP by Reducing Cu Catalyst Concentration. *Macromolecules* **2013**, *46* (3), 683-691.
51. Matyjaszewski, K.; Woodworth, B. E., Interaction of Propagating Radicals with Copper(I) and Copper(II) Species. *Macromolecules* **1998**, *31* (15), 4718-4723.
52. Poli, R., Relationship between One-Electron Transition-Metal Reactivity and Radical Polymerization Processes. *Angewandte Chemie International Edition* **2006**, *45* (31), 5058-5070.
53. Allan, L. E. N.; Perry, M. R.; Shaver, M. P., Organometallic mediated radical polymerization. *Progress in Polymer Science* **2012**, *37* (1), 127-156.
54. Wayland, B. B.; Peng, C.-H.; Fu, X.; Lu, Z.; Fryd, M., Degenerative Transfer and Reversible Termination Mechanisms for Living Radical Polymerizations Mediated by Cobalt Porphyrins. *Macromolecules* **2006**, *39* (24), 8219-8222.

55. Wang, F.-S.; Yang, T.-Y.; Hsu, C.-C.; Chen, Y.-J.; Li, M.-H.; Hsu, Y.-J.; Chuang, M.-C.; Peng, C.-H., The Mechanism and Thermodynamic Studies of CMRP: Different Control Mechanisms Demonstrated by Coll(TMP), Coll(salen*), and Coll(acac)₂ Mediated Polymerization, and the Correlation of Reduction Potential, Equilibrium Constant, and Control Mechanism. *Macromolecular Chemistry and Physics* **2016**, 217 (3), 422-432.
56. Debuigne, A.; Poli, R.; Jérôme, C.; Jérôme, R.; Detrembleur, C., Overview of cobalt-mediated radical polymerization: Roots, state of the art and future prospects. *Progress in Polymer Science* **2009**, 34 (3), 211-239.
57. Soerensen, N.; Schroeder, H.; Buback, M., SP–PLP–EPR Measurement of CuII-Mediated ATRP Deactivation and CuI-Mediated Organometallic Reactions in Butyl Acrylate Polymerization. *Macromolecules* **2016**, 49 (13), 4732-4738.
58. Ribelli, T. G.; Rahaman, S. M. W.; Daran, J.-C.; Krys, P.; Matyjaszewski, K.; Poli, R., Effect of Ligand Structure on the CuII–R OMRP Dormant Species and Its Consequences for Catalytic Radical Termination in ATRP. *Macromolecules* **2016**, 49 (20), 7749-7757.
59. Pan, X.; Tasdelen, M. A.; Laun, J.; Junkers, T.; Yagci, Y.; Matyjaszewski, K., Photomediated controlled radical polymerization. *Progress in Polymer Science* **2016**, 62, 73-125.
60. Williams, V. A.; Ribelli, T. G.; Chmielarz, P.; Park, S.; Matyjaszewski, K., A Silver Bullet: Elemental Silver as an Efficient Reducing Agent for Atom Transfer Radical Polymerization of Acrylates. *Journal of the American Chemical Society* **2015**, 137 (4), 1428-1431.
61. De Paoli, P.; Isse, A. A.; Bortolamei, N.; Gennaro, A., New insights into the mechanism of activation of atom transfer radical polymerization by Cu(I) complexes. *Chemical Communications* **2011**, 47 (12), 3580-3582.
62. Krys, P.; Wang, Y.; Matyjaszewski, K.; Harrisson, S., Radical Generation and Termination in SARA ATRP of Methyl Acrylate: Effect of Solvent, Ligand, and Chain Length. *Macromolecules* **2016**, 49 (8), 2977-2984.
63. Wang, Y.; Zhong, M.; Zhang, Y.; Magenau, A. J. D.; Matyjaszewski, K., Halogen Conservation in Atom Transfer Radical Polymerization. *Macromolecules* **2012**, 45 (21), 8929-8932.
64. Fantin, M.; Isse, A. A.; Bortolamei, N.; Matyjaszewski, K.; Gennaro, A., Electrochemical approaches to the determination of rate constants for the activation step in atom transfer radical polymerization. *Electrochimica Acta* **2016**, 222, 393-401.
65. Kaur, A.; Ribelli, T. G.; Schröder, K.; Matyjaszewski, K.; Pintauer, T., Properties and ATRP Activity of Copper Complexes with Substituted Tris(2-pyridylmethyl)amine-Based Ligands. *Inorganic Chemistry* **2015**, 54 (4), 1474-1486.
66. Nikitin, A. N.; Hutchinson, R. A.; Wang, W.; Kalfas, G. A.; Richards, J. R.; Bruni, C., Effect of Intramolecular Transfer to Polymer on Stationary Free-Radical Polymerization of Alkyl Acrylates, 5 – Consideration of Solution Polymerization up to High Temperatures. *Macromolecular Reaction Engineering* **2010**, 4 (11-12), 691-706.

ToC Graphic

